2024 European Control Conference (ECC)
June 25-28, 2024. Stockholm, Sweden

Body-aware Local Navigation for Asymmetric Holonomic Robots using Control Barrier Functions

Akshit Saradagi[1], Scott Fredriksson, Anton Koval and George Nikolakopoulos

***Abstract*— In this article, we propose a body-aware local navigation strategy for asymmetric holonomic robots for collision-free navigation in narrow pathways with sharp turns. In such scenarios, a robot with non-circular or asymmetric footprint that is comparable to the dimension of the pathways collides with walls when tracking Voronoi paths or risk-aware paths. This problem is addressed in this article through a novel multi-control barrier functions (CBF) based control strategy that achieves the objective of safe collision-free maneuvering at sharp turns. The proposed method is significantly computationally light in comparison to approaches based on model predictive control and online occupancy-grid based free-space and collision detection. In the proposed approach, a minimal set of parameters that characterize a sharp turn and the robot footprint are used to define six control barrier functions that define safe and unsafe regions of operation for a robot. A quadratic programming based CBF safety filter is designed that takes a nominal goal-reaching control as input and returns a minimally-deviating output that enforces the control barrier constraints and renders the safe set forward invariant throughout the turning maneuver. The three kinematic control inputs of the holonomic robot are shared in a conflict-free manner among the six control barrier constraints. The proposed local navigation approach was thoroughly validated in multiple scenarios in a simulated environment, where a robot with asymmetric footprint achieves collision-free maneuvering along multiple sharp turns, while respecting the safety and actuation constraints.**

I. INTRODUCTION

The capability of robots to operate in challenging environments is being pushed everyday, with applications such as search and rescue operations, autonomy in mines and operation in busy human-robot cohabited spaces presenting inspiring challenges. In such applications, the autonomous robots and vehicles are expected to navigate through cluttered environments while being aware of their physical footprints. In robotics, Voronoi paths [1] and risk-aware planning [2] methods are generally used to plan safe paths, under the crucial assumption that the robot has a circular/symmetrical footprint and the scale of the environment is considerably larger than the footprint of the robot. In this sense, such algorithms are not body-aware and cannot be directly used by asymmetrical robots in cluttered environments. For instance, in scenarios where the length of the intersections and pathways are comparable to the footprint of the robot.

Designing body-aware algorithms is a primary problem for several robots, such as large mining vehicles, trailer-truck systems, aerial manipulators, quadruped robots navigating in constrained indoor environments and multi-robot formations that collaboratively execute tasks in constrained environments. Body-aware algorithms provide several advantages for such robots, some of which are illustrated in Figure 1. In the single agent case, body-aware navigation and control expands the reach of an agent, thus reducing the costs of travel in cluttered environments. In a heterogeneous multi-agent task allocation scenario, agents of the fleet can be optimally routed to target locations, by taking their footprints into account. Traditionally, Voronoi paths (loci of equidistant points from occupied spaces) and risk-aware path planning are employed for safe navigation. Such methods are designed under the assumption that a robot has symmetrical footprint, with the traversibility question decided by whether or not the width of the passage is larger than the largest dimension of the robot. This is a conservative approach that limits the reach of a robot in confined spaces and moreover, robots with asymmetrical footprints encounter collisions when using such methods.

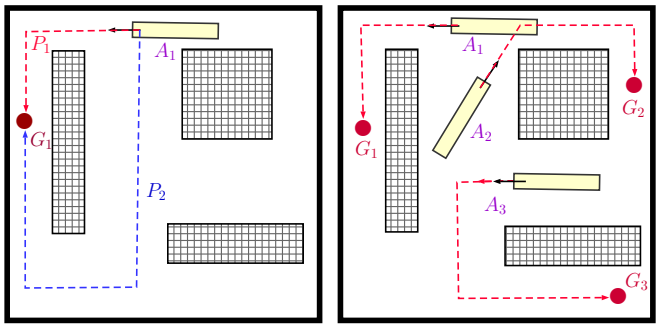

Fig. 1: Advantages of body-aware planning and navigation. a) Body-aware planning and navigation expands the reach of an agent, thus reducing the costs of travel in cluttered environments. For instance, the robot must choose path P_1 over P_2, as the cost of P_1 is less than P_2. b) In a heterogeneous multi-agent task allocation scenario, agents A_i of the fleet can be optimally routed to target locations G_i, based on the costs that take the robot footprint into account.

Existing methods on body-aware navigation for asymmetric robots can be classified into three broad categories [3]: 1) Artificial potential field based methods such as [4], where multiple sensors are placed on the perimeter of the robot, whose data is processed to derive attractive and repulsive forces. 2) Model predictive control-based methods such as

[1] Corresponding author
The authors are with the Robotics and AI Group, Department of Computer Science, Electrical and Space Engineering, Luleå University of Technology, Sweden. Emails: akssar@ltu.se; scofre@ltu.se; antkov@ltu.se; geonik@ltu.se

[5] [6] [7], where the model of a robot is propagated in a finite prediction horizon to find collision-free trajectories. Such methods look to solved nonlinear and nonconvex optimization problems and are computationally expensive. 3) Occupancy grid based methods that view the problem as a path planning problem, such as [8] [9] [10] [11], where the occupancy grids are processed using computationally intense operations (such as convolution with the robot footprint) to find collision-free configurations.

The following are the contributions of the article with respect to the state-of-the-art. We propose a novel control barrier functions based control strategy for holonomic robots with asymmetric footprints that achieves body-aware maneuvering at sharp turns. In maneuvering at a sharp turn, the robot's footprint must be restricted inside a non-convex region, which is difficult to model as constraints for an optimization problem. In this article, we present a formulation which overcomes this difficulty, by defining body-aware robot-centric constraints. Here, the points defining the sharp turn are constrained to be within linear subspaces defined by the footprint of the robot. These subspaces characterize the body-aware safe region of operation for a robot and are used to define control barrier functions. The proposed method is suitable for real-time online implementation, as a simple quadratic program with three decision variables and six linear inequality constraints is solved at every instant of the turning maneuver, to derive safe control inputs. This approach requires significantly lower computation than model predictive control [5] (nonlinear predictions with nonconvex constraints in this case) and occupancy grid-based methods (involving operations such as convolution with the robot footprint) [10]. We present a thorough simulation based validation of the proposed strategy and investigate the effect of CBF parameters, the length of the robot and initial configuration of the robot on the performance during the turning maneuver.

II. Problem formulation

In this article, a holonomic ground robot with omni-directional mobility is considered. The triple $(x_r, y_r, \theta_r) \in \mathbb{R}^2 \times \mathbb{S}^1$ represents the position and orientation of the robot on a plane. The robot is considered to have an asymmetric footprint that can be contained inside a rectangle (shown in Figure 2), with L being the length along the longer dimension of the robot. d_l represents the safety margin along the length of the robot and $2 \times d_b$ represents the width of the robot inclusive of the safety margins. We assume that $2 \times d_b \ll L$. In this setting, the footprint of the robot is defined by the following four points.

$$
\begin{aligned}
P_r^1 &= (x_r + d_l\cos(\theta_r) - d_b\sin(\theta_r), y_r + d_l\sin(\theta_r) + d_b\cos(\theta_r)) \\
P_r^2 &= (x_r - L\cos(\theta_r) - d_l\cos(\theta_r) - d_b\sin(\theta_r), \\
&\qquad y_r - L\sin(\theta_r) - d_l\sin(\theta_r) + d_b\cos(\theta_r)) \\
P_r^3 &= (x_r - L\cos(\theta_r) - d_l\cos(\theta_r) + d_b\sin(\theta_r), \\
&\qquad y_r - L\sin(\theta_r) - d_l\sin(\theta_r) - d_b\cos(\theta_r)) \\
P_r^4 &= (x_r + d_l\cos(\theta_r) + d_b\sin(\theta_r), y_r + d_l\sin(\theta_r) - d_b\cos(\theta_r))
\end{aligned} \tag{1}
$$

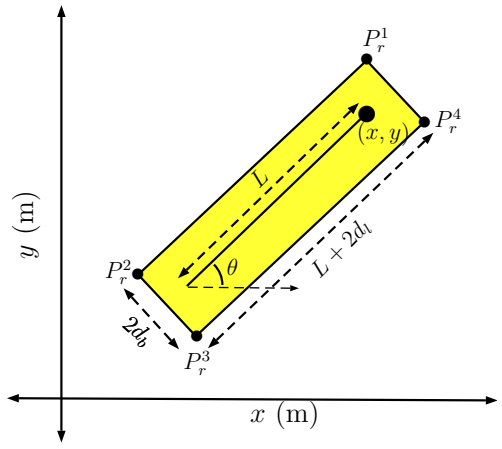

Fig. 2: Schematic of an asymmetric holonomic robot, showing the robot states & the parameters of the robot footprint.

In this article, we are looking to design a body-aware turning maneuver for an asymmetric robot to pass through a narrow turn. The parameters that minimally characterize a narrow turn are shown in Figure 3. The lines $L_c^1(x,y) = l_{11}x + l_{12}y + c_1 = 0$ and $L_c^2(x,y) = l_{21}x + l_{22}y + c_1 = 0$, which meet at the point P_c^1 define the outer perimeter of the turn. Two lines, parallel to L_c^1 and L_c^2 and meeting at a point P_c^2 define the inner boundary of the turn. A point P_c^3 on the inner perimeter that is parallel to the line L_c^1 will also be used in the formulation.

In passing through a narrow turn to reach the goal location G_1, the footprint of the robot must be restricted within the region contained between the inner and outer perimeter of the turn. The locus of equidistant points between the inner and outer perimeters of the turn is referred to as the Voronoi path. When an asymmetric robot attempts to track the Voronoi path, there are locations where the robot cannot escape collisions with the walls. This motivates the need to develop body-aware local navigation for robots with asymmetric footprints. In this article, we propose a computationally light methodology that generates collision-free trajectories for an asymmetric holonomic robot that requires minimal information about a narrow turn (lines $L_c^1(x,y) = 0$, $L_c^2(x,y) = 0$ and points (P_c^1, P_c^2, P_c^3)).

III. Methodology

A. Control Architecture

In this article, the control architecture shown in Figure 4 is used to control a holonomic mobile robot whose state $(x_r, y_r, \theta_r) \in \mathbb{R}^2 \times \mathbb{S}^1$ evolves in accordance with the kinematic model:

$$
\begin{bmatrix} \dot{x}_r \\ \dot{y}_r \\ \dot{\theta}_r \end{bmatrix} = \begin{bmatrix} v_x \\ v_y \\ \omega_z \end{bmatrix} \tag{2}
$$

where, $[v_x \;\; v_y]^\top \in \mathbb{R}^2$ and $\omega_z \in \mathbb{R}$ are the robot's linear and angular velocities respectively. We base our control barrier functions based control design on the above kinematic model of the robot and assume the existence of a high-fidelity inner-loop controller that is capable of tracking the prescribed

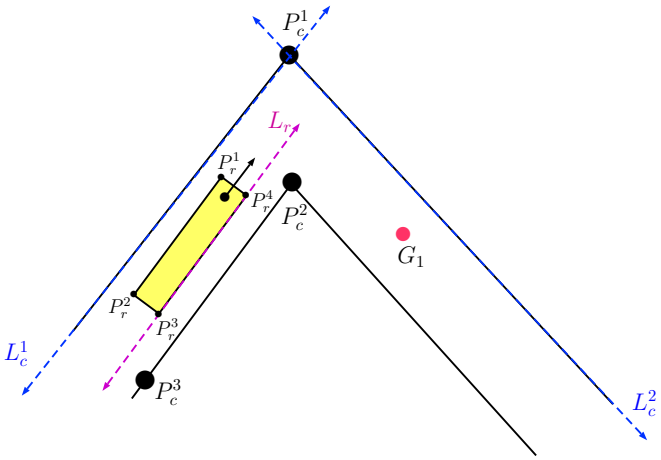

Fig. 3: The environment around a narrow turn is characterized by the points (P_c^1, P_c^2, P_c^3) and the lines (L_c^1) and L_c^2.

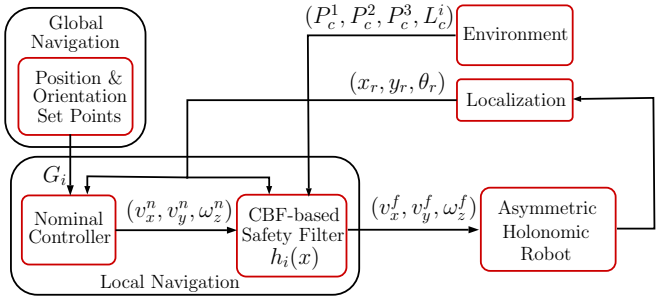

Fig. 4: Block diagram of the control architecture.

velocities. It is assumed that a global navigator/planner sets the goal locations G_i for the robot after a turn and the parameters characterizing the turn are known. In an experimental scenario, these parameters can be derived by processing the outputs of a 2D LiDAR. The CBF-based local navigation strategy, which constitutes the main contribution of this article, is presented in the following two subsections.

B. Control Barrier Functions (CBFs) for safe navigation

The constraints involved in a turning maneuver at a narrow turn are illustrated in Figure 3. The robot's footprint must always remain in the region between the inner and outer perimeter of the narrow turn, which is a non-convex region. Constraints with respect to the outer walls are simple to model: the robot must remain within the convex region whose boundary is defined by lines L_c^1 and L_c^2. The real challenge lies in capturing the constraints with respect to the inner walls: the robot must remain outside the inner walls, which is a non-convex region as it cannot be modelled as the intersection of half-spaces. In this article, we take an unconventional body-centric approach and propose to model this constraint in the following manner: the points P_c^2 and P_c^3 must remain below the line L_r that passes through points P_r^3 and P_r^4 that define the footprint of the robot (shown as a dashed magenta line in Figure 3). In this way, constraints with respect to the inner wall are captured through two subspace constraints. In conjunction with the CBF-based navigation approach (to be presented in section III-C), the two constraint suffice in capturing the constraints with respect to the inner perimeter of the turn.

Next, we use the constraints described so far, to define a safe region of operation in the robot's state space. When moving from the robot's current location (x_r, y_r, θ_r) to the goal location G_1, collision-free turning maneuver is ensured if the robot's footprint (defined by P_r^i, $i \in \{1,\dots,4\}$ and shown in Figure 2) meets the following constraints:

1) $L_c^1(P_r^1) \leq 0$ and $L_c^1(P_r^2) \leq 0$ which define the control barrier functions

$$h_1(x_r, y_r, \theta_r) = -L_c^1(P_r^1) \text{ and } h_2(x_r, y_r, \theta_r) = -L_c^1(P_r^2). \tag{3}$$

2) $L_c^2(P_r^1) \leq 0$ and $L_c^2(P_r^2) \leq 0$ which define the control barrier functions

$$h_3(x_r, y_r, \theta_r) = -L_c^2(P_r^1) \text{ and } h_4(x_r, y_r, \theta_r) = -L_c^2(P_r^2). \tag{4}$$

3) Let $L_r(x,y) = l_{r1}x + l_{r2}y + c_r = 0$ be the line passing through the points P_r^3 and P_r^4, which are the points defining the extremities of the robot's footprint. In the robot's turning maneuver, the following constrains are imposed: $L_r(P_c^2) \leq 0$ and $L_r(P_c^3) \leq 0$, which define the barrier functions

$$h_5(x_r, y_r, \theta_r) = -L_r(P_c^2) \text{ and } h_6(x_r, y_r, \theta_r) = -L_r(P_c^3). \tag{5}$$

If the functions $\{h_1,\dots,h_6\}$ are maintained greater than zero, throughout the turning maneuver, that is

$$h_i(x_r, y_r, \theta_r) \geq 0 \quad \forall\, t \geq 0,\ \forall\, i \in \{1,\dots,6\} \tag{6}$$

the robot reaches the goal position, without any collisions with the walls. The set

$$\mathscr{S} = \{(x_r, y_r, \theta_r) \in \mathbb{R}^2 \times \mathbb{S}^1 \mid h_i(x_r, y_r, \theta_r) \geq 0, i \in \{1,\dots,6\}\} \tag{7}$$

defines the set of collision-free configurations for the robot. Note that the constraints have been defined for a right turn relative to the robots current pose, and the same constraints hold for a left turn, with P_r^1 and P_r^2 exchanging positions with P_r^3 and P_r^4.

Next, we recall some preliminaries concerning control barrier functions (CBFs) from [12], which will be used in the rest of this article to design the novel local navigation strategy for a holonomic mobile robot that ensures safety throughout the turning maneuver. The ideas will be defined by considering a control-affine dynamical system

$$\dot{x} = f(x) + g(x)u, \quad x \in \mathscr{X} \subset \mathbb{R}^n, u \in \mathscr{U} \subset \mathbb{R}^m \tag{8}$$

where f and g are Lipschitz continuous functions. Let $\mathscr{S} \subset \mathscr{X}$ be the region of the state-space, which is deemed as a safe region for the operation of (8). Let $h(x) : \mathscr{D} \subset \mathscr{X} \to \mathbb{R}$ be a continuously differentiable function, with $\mathscr{S} \subset \mathscr{D}$, such that $\mathscr{S} := \{x \in \mathscr{X} \mid h(x) \geq 0\}$, that is, $\mathscr{S}$ is a zero super-level set of the function $h(x)$. Note that the six functions in (3)-(5) are defined such that the associated safe sets are the

zero super-level sets of the functions. The set $\mathscr{S}$ is rendered safe if the control input to (8) ensures positive invariance of the set $\mathscr{S}$, that is, $x(t_0) \in \mathscr{S}$ implies $x(t) \in \mathscr{S}$ for all $t \geq t_0$. In addition, if $\mathscr{S}$ is rendered asymptotically stable, when the systems is initialized in $\mathscr{D} \setminus \mathscr{S}$, a measure of robustness can be incorporated into the notion of safety. The following definition introduces the notion of a control barrier function and presents a condition, the verification of which ensures the safety of the dynamical system (8).

Definition 1 (A control barrier function [12]): A continuously differentiable function $h(x) : \mathscr{D} \to \mathbb{R}$ is a control barrier function, if there exists a real parameter $\gamma > 0$ and an extended class-$\mathscr{K}$ function α, such that for all $x \in \mathscr{D}$,

$$\sup_{u \in \mathscr{U}} \left\{ L_f h(x) + L_g h(x) u + \gamma \alpha(h(x)) \right\} \geq 0, \tag{9}$$

where an extended class-$\mathscr{K}$ function is a continuous function $\alpha : [-b, a) \to [0, \infty)$, with $a, b \in (0, \infty)$, that is strictly increasing and $\alpha(0) = 0$.

The forward invariance of $\mathscr{S}$ ($\dot{h} \geq 0$ on $\partial\mathscr{S}$) and asymptotic stability of $\mathscr{S}$ ($\dot{h} > 0$ in $\mathscr{D} \setminus \mathscr{S}$) are captured together in the condition (9). The existence of at least one input from the admissible set $\mathscr{U}$, which renders (9) feasible, enables the design of a control input that ensures safety of the dynamical system (8). Since the verification of the validity of the CBFs $h_1, \ldots, h_6$ can be performed as in the article [13], we do not present this verification in this article and redirect the focus on the design aspects.

C. Quadratic programming based CBF safety filter

In this section, we present the CBF-based control design that ensures that the six control barrier functions are maintained greater then zero through out the turning maneuver.

In the CBF approach, a quadratic programming based control filter is designed, which takes a nominal controller $u_{\text{nom}}(x(t))$ as input and yields a minimally deviating filtered control input $u^*(x)$ that enforces the safety constraints (6). In this work, we use a linear proportional controller

$$\begin{aligned} u_{\text{nom}}(x) &= [v_x^n \;\; v_y^n \;\; \omega_z^n]^\top \\ &= [-p_1(x_r - G_x) \; - p_2(y_r - G_y) \; - p_3(\theta_r - G_\theta)]^\top \end{aligned} \tag{10}$$

with the gains $p_i > 0$, as the nominal controller for the robot kinematics (2). This simple nominal controller has been designed to reach a goal configuration $G = (G_x, G_y, G_\theta)$ after the turn with no consideration for the safety constraints, and exponentially drives the robot to the goal location G with the robot aligned at the angle G_θ. The CBF approach takes such a nominal controller and filters it to yield a controller $u^*(x)$ that ensures the robot always remains in the safe zone.

As the functions $h_i(x)$ are CBFs, for a fixed x, each of the constraints (9) are feasible linear constraints. The filtered control $u^*(x) = (v_x^f, v_y^f, \omega_z^f)$ is derived by solving the following minimum-norm Quadratic program

$$\begin{aligned} u^*(x) &= \arg\min_{u \in \mathscr{U}} ||u - u_{\text{nom}}(x)||^2 \\ \text{subject to} \;:\; & L_f h_i(x) + L_g h_i(x) u \geq -k_1 \alpha(h_i(x)), \\ & i \in \{1, \ldots 6\}. \end{aligned} \tag{11}$$

The classical Quadratic program (11) with the quadratic cost and linear constraints in the decision variable $u = \{v_x, v_y, \omega_z\}$ can be efficiently solved at every sampling instant. When the controller $u^*(x)$ is Lipschitz continuous, the forward invariance of the set $\mathscr{S}$ and it's asymptotic stability from the corresponding set $\mathscr{D} \setminus \mathscr{S}$ can be established using Comparison Lemma as in [12].

The nominal controller and the safety filter are part of the local navigation module in Figure 4. This module takes as input, the way-point after the corridor G_1, the parameters defining a turn and the current pose of the robot (x_r, y_r, θ_r). The filtered velocity commands from the CBF filter are either used directly as input to a robot or set as references to a velocity tracking controller.

D. Control sharing among multiple barrier functions

In the optimization problem (11), the three control inputs (v_x, v_y, ω_z) of the robot are being shared in establishing six control barrier constraints. In general, in a multi-control barrier function scenario, it is required that the control sharing be valid in establishing both forward invariance of the safe sets and asymptotic stability of the safe sets. In this work, it is only required that the safe set S in (7), which is the intersection of the safe sets associated with the six barrier functions, be rendered forward invariant for all time. To this end, the guarantees for conflict-free input sharing among multiple barrier functions to render a safe set forward invariant were established in the work [13]. The same guarantees hold for the input-sharing scenario in the optimization problem (11) of this article.

IV. Validation of the proposed algorithm

In this section, we present a simulation-based validation of the proposed body-aware local navigation strategy.

A. Validation scenario I

The first is an illustrative scenario, where a holonomic robot with a skewed rectangular footprint maneuvers through a narrow turn safely, to reach a goal position with no collisions. The robot has a rectangular footprint of length (L) 3m with a safety margin (d_l) of 0.25m and width ($2 * d_b$) of 0.7m. The longest dimension of the robot footprint is $L + 2 \times d_l = 3.5$m. A narrow right-angle turn is considered, where the corridors leading to the turn and after the turn have a width of 2m. In Figure 5, it is clear that if the robot tracks the Voronoi path, there is no way to avoid collision with the walls. To illustrate the simplicity of the proposed method, we chose a proportional controller (10) as the nominal controller in the CBF filter with $p_i = 0.1$, that tracks the waypoint (-0.25m, 3m, 0rad) set by a global navigator. The six CBFs (described in section II) are constructed and the associated constraints are set as inequality constraints for the CBF filter (11) with the constants $k_i = 0.1, i \in \{1, \ldots, 6\}$. The absolute values of the linear and turning velocities of the robot are upper bounded by 0.2m/s and 0.25rad/s respectively. The parameters characterizing the turn (the points P_c^1, P_c^2 and the lines L_c^1 and L_c^2) are assumed to be known. In an experimental

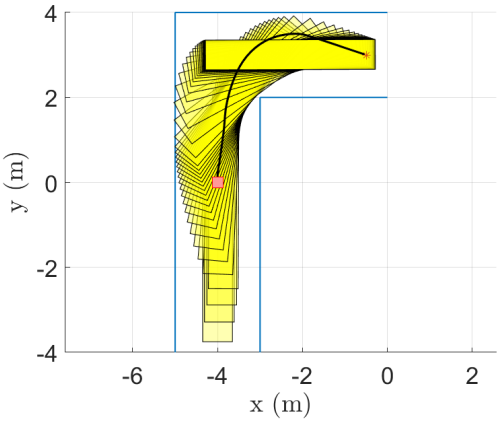

Fig. 5: The turning maneuver executed by the robot using the proposed local navigation algorithm.

scenario, these parameters can be derived by processing the outputs of a 2D LiDAR.

In Figure 5, we show the path taken by the robot to successfully maneuver through a narrow turn, with the footprint of the robot overlayed on it. In Figures 6a and 6b, the evolution of the control barrier functions ($h_1 \ldots h_6$) and the control inputs $(v_x^f, v_y^f, \omega_z^f)$ derived from the CBF filter are plotted respectively. Through out the turning maneuver, the control barrier functions are maintained above zero and the control inputs within the desired bounds. In Figure 7a, we plot the trajectories taken by the robot from different initial configurations in reaching its goal position. In Figure 7b, the trajectories taken by robots of different lengths (L) with fixed d_l and d_b are plotted. It can be seen that the robot successfully executes safe turning maneuvers for the all the cases considered in Figures 7a and 7b.

B. Validation Scenario II

Here, we consider a more complex scenario, where we demonstrate the utility of the proposed local navigation approach in a larger mission. A maze comprising of seven turns is considered and shown in Figure 8, that consists of both left and right turns and turning angles including right, acute and obtuse angles. The parameters describing the robot, and the CBF filter are the same as in the first validation scenario. It is assumed that a global planner supplies the robot with way points (indicated with *) to reach along the maze. In straight sections of the maze far from turns, the robot does not face collision when tracking Voronoi paths and the robot can use a waypoint tracking controller as the nominal controller to track the voronoi path (indicated as a dashed blue line) that passes through the goal locations. When the robot nears a sharp turn, the proposed local navigation solution is invoked, so that the robot deviates from the voronoi path and executes the body-aware turning maneuver proposed in this work. The validation of this navigation strategy is shown in Figures 8 and 9, where the robot successfully reaches seven goal locations set by a global navigator, while executing body-aware turning maneuvers at seven narrow turns.

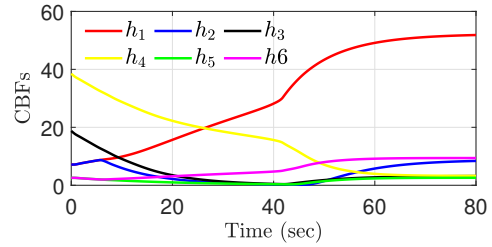

(a) Evolution of the control barrier functions $h_i(x(t))$.

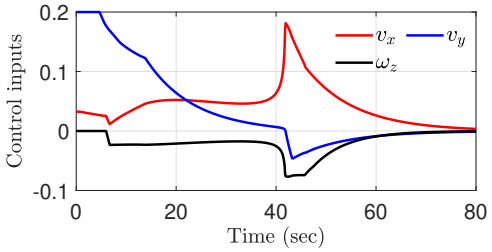

(b) Evolution of the control inputs derived from the CBF filter.

Fig. 6: Simulation based validation of the proposed local navigation strategy.

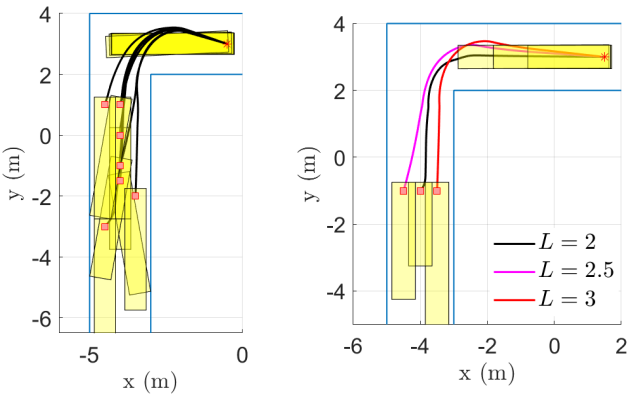

(a) (b)

Fig. 7: Turning maneuvers (a) from different initial conditions and (b) for robots with different lengths (L).

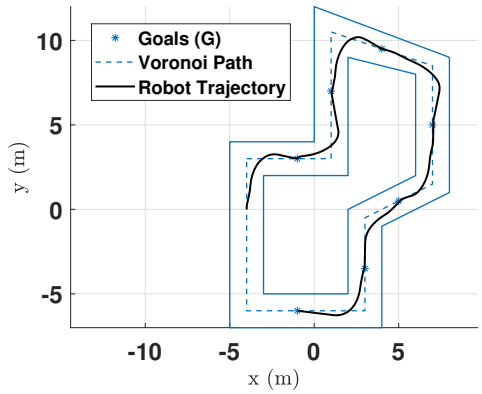

Fig. 8: Validation scenario II. Tracking goal locations in a maze with left/right turns with acute, obtuse and right angles.

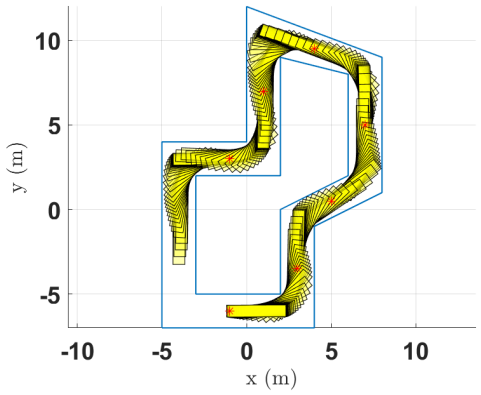

Fig. 9: In the second validation scenario, the footprint of the robot is contained within the maze throughout the mission.

C. Discussion and Comparison

In this subsection, we present a qualitative comparison between the proposed method and finite horizon Nonlinear Model Predictive Control (NMPC) that utilizes the constraints formulated in this article. **1) Complexity of the optimization problem.** Both the methods solve the local navigation problem through an optimization problem. In the proposed method, a quadratic program with three decision variables, comprising of a quadratic cost function and linear inequality constraints is solved. In NMPC, a nonlinear and nonconvex problem is solved, that comprises of quadratic cost and nonlinear equality constraints and nonlinear and nonconvex inequality constraints. The number of decision variables and the nonlinearity associated with the problem grows with the length of the prediction horizon. **Optimality of the turning maneuver.** The proposed method offers a reactive solution that may not be optimal with respect to the length of the path, time or the control effort. NMPC provides a local optimal solution when the solution exists, as it explicitly accounts for the state and actuation costs, but at extremely high computational costs. 3) **Tuning of the design parameters.** Both the methods involve a tuning process. In the proposed method, the gains of the nominal controller and the CBF parameters have to be tuned to obtain the desired performance. In finite horizon NMPC, the length of the planning horizon and the stage and terminal costs have to be tuned to extract the desired performance. 4) **Feasibility of the turning maneuver.** In the proposed method, the robot encounters a deadlock scenario, when a safe turning maneuver is infeasible. In NMPC, infeasibility of the turning maneuver is reflected as infeasibility of the optimization problem. When using small planning horizons, NMPC faces deadlock situations and may not reach the goal location, just as in the proposed method.

V. CONCLUSIONS

In this article, we presented a body-aware local navigation algorithm for asymmetric holonomic mobile robots. By taking into account the footprint of the robot and a minimal set of parameters characterizing a narrow turn, six control barrier functions were formulated that define the safe zone of operation for a robot. The robot was restricted to the safe zone by filtering a nominal goal reaching controller to derive a minimally-invasive control that guarantees safety as defined by the control barrier functions. We presented a simulation-based validation of the proposed local navigation strategy, where a long asymmetrical robot successfully passed through narrow turns to reach desired goal locations. A thorough analysis of the performance of the algorithm was conducted, with respect to parameters such as the CBF constants, the length of the robot and different initializations of the robot. The approach was also integrated into a larger mission, where the robot successfully navigated through a narrow circuit comprising of seven sharp turns. In the future, we look to experimentally validate the proposed solution, by developing an online solution, where the parameters of the intersection are computed online using LiDAR measurements.

REFERENCES

[1] H. Choset and J. Burdick, "Sensor-Based Exploration: The Hierarchical Generalized Voronoi Graph," vol. 19, no. 2, pp. 96–125.

[2] S. Karlsson, A. Koval, C. Kanellakis, and G. Nikolakopoulos, "D^*_+: A risk aware platform agnostic heterogeneous path planner," *Expert Systems with Applications*, vol. 215, p. 119408, Apr. 2023.

[3] I. Mir, F. Gul, S. Mir, M. A. Khan, N. Saeed, L. Abualigah, B. Abuhaija, and A. H. Gandomi, "A survey of trajectory planning techniques for autonomous systems," *Electronics*, vol. 11, no. 18, 2022.

[4] B. Holt, J. Borenstein, Y. Koren, and D. Wehe, "Omninav: Obstacle avoidance for large, non-circular, omnidirectional mobile robots," *Robotics and Manufacturing*, vol. 6, pp. 27–30, 1996.

[5] J. J. Park, C. Johnson, and B. Kuipers, "Robot navigation with mpepc in dynamic and uncertain environments: From theory to practice," in *IROS 2012 Workshop on Progress, Challenges and Future Perspectives in Navigation and Manipulation Assistance for Robotic Wheelchairs*, 2012.

[6] D. J. Gonon, D. Paez-Granados, and A. Billard, "Reactive navigation in crowds for non-holonomic robots with convex bounding shape," *IEEE Robotics and Automation Letters*, vol. 6, no. 3, pp. 4728–4735, 2021.

[7] A. Hornung, M. Phillips, E. Gil Jones, M. Bennewitz, M. Likhachev, and S. Chitta, "Navigation in three-dimensional cluttered environments for mobile manipulation," in *2012 IEEE International Conference on Robotics and Automation*, pp. 423–429, 2012.

[8] B. MacAllister, J. Butzke, A. Kushleyev, H. Pandey, and M. Likhachev, "Path planning for non-circular micro aerial vehicles in constrained environments," in *2013 IEEE International Conference on Robotics and Automation*, pp. 3933–3940, 2013.

[9] M. Dakulović, C. Sprunk, L. Spinello, I. Petrovic, and W. Burgard, "Efficient navigation for anyshape holonomic mobile robots in dynamic environments," in *2013 IEEE/RSJ International Conference on Intelligent Robots and Systems*, pp. 2644–2649, 2013.

[10] R. Samaniego, J. Lopez, and F. Vazquez, "Path planning for non-circular, non-holonomic robots in highly cluttered environments," *Sensors*, vol. 17, no. 8, 2017.

[11] B. Lau, C. Sprunk, and W. Burgard, "Efficient grid-based spatial representations for robot navigation in dynamic environments," *Robotics and Autonomous Systems*, vol. 61, no. 10, pp. 1116–1130, 2013.

[12] A. D. Ames, S. Coogan, M. Egerstedt, G. Notomista, K. Sreenath, and P. Tabuada, "Control barrier functions: Theory and applications," in *2019 18th European Control Conference (ECC)*, pp. 3420–3431, 2019.

[13] A. Saradagi, A. Banerjee, S. Satpute, and G. Nikolakopoulos, "Safe autonomous docking maneuvers for a floating platform based on input sharing control barrier functions," in *2022 IEEE 61st Conference on Decision and Control (CDC)*, pp. 3746–3753, 2022.